Organization of Monoterpene Biosynthesis in Mentha. Immunocytochemical Localizations of Geranyl Diphosphate Synthase, Limonene-6-Hydroxylase, Isopiperitenol Dehydrogenase, and Pulegone Reductase[1]

Glenn W. Turner and Rodney Croteau*

Institute of Biological Chemistry, Washington State University, Pullman, Washington 99164

We present immunocytochemical localizations of four enzymes involved in *p*-menthane monoterpene biosynthesis in mint: the large and small subunits of peppermint (*Mentha x piperita*) geranyl diphosphate synthase, spearmint (*Mentha spicata*) (−)-(4*S*)-limonene-6-hydroxylase, peppermint (−)-trans-isopiperitenol dehydrogenase, and peppermint (+)-pulegone reductase. All were localized to the secretory cells of peltate glandular trichomes with abundant labeling corresponding to the secretory phase of gland development. Immunogold labeling of geranyl diphosphate synthase occurred within secretory cell leucoplasts, (−)-4*S*-limonene-6-hydroxylase labeling was associated with gland cell endoplasmic reticulum, (−)-trans-isopiperitenol dehydrogenase labeling was restricted to secretory cell mitochondria, while (+)-pulegone reductase labeling occurred only in secretory cell cytoplasm. We discuss this pathway compartmentalization in relation to possible mechanisms for the intracellular movement of monoterpene metabolites, and for monoterpene secretion into the extracellular essential oil storage cavity.

Monoterpenes are a large and diverse class of volatile C_{10} isoprenoids that are the major constituents of many plant essential oils and resins. These natural products play important chemoecological roles in the interactions of plants with their environments. Some monoterpenes have been implicated as allelopathic agents, and they often directly, or indirectly, protect plants from herbivores and pathogens (Pickett, 1991; Harborne, 1991; Langenheim, 1994; Wise and Croteau, 1999; Hallahan, 2000). As important constituents of floral scents, monoterpenes also function to attract pollinators (Dudareva and Pichersky, 2000). Some plants release volatile monoterpenes and sesquiterpenes in response to herbivore damage that function to attract predatory insects that in turn feed on, or parasitize, the herbivorous insects (Langenheim, 1994; Degenhardt et al., 2003). In conifer species, mechanical wounding, insect attack, or applications of methyl jasmonate can induce resin secretion and differentiation of traumatic resin ducts within wounded tissues, producing a protective barrier of resin at the site of wounding (Steele et al., 1995; Trapp and Croteau, 2001; Franceschi et al., 2002; Martin et al., 2002). Many plant species constitutively produce large quantities of terpenoid-rich resins and essential oils within specialized glandular tissues, such as glandular trichomes, secretory cavities, and secretory ducts (Fahn, 1979, 2000). These natural stores of plant terpenoids probably serve as deterrents to herbivorous insects, but they also provide commercially important sources of flavorings, fragrances, resins, and pharmaceuticals (Langenheim, 1994; Wise and Croteau, 1999). The glandular cells of these secretory tissues are of interest for their remarkable ability to rapidly generate substantial amounts of specific terpenoid products.

Peppermint (*Mentha x piperita*) has been employed as a model system for the study of monoterpene biosynthesis (Wise and Croteau, 1999). The peltate glandular trichomes (peltate glands) of peppermint produce copious amounts of a commercially valuable, menthol-rich essential oil, composed primarily of *p*-menthane monoterpenes. These structures consist of eight glandular cap cells, a stalk cell, and a basal cell (Fig. 1). A protocol for isolating and purifying secretory cells from these trichomes has provided an enriched source of monoterpene biosynthetic enzymes and their corresponding transcripts (McCaskill et al., 1992; Wise and Croteau, 1999), an advance that has resulted in the cloning of nearly all of the genes and characterization of the corresponding enzymes of the pathway to (−)-menthol from the primary metabolites isopentenyl diphosphate (IPP) and dimethylallyl diphosphate (DMAPP; Fig. 2). The ultrastructure of the peppermint glandular cells appears typical of plant essential oil and resin secreting cells, with numerous amoeboid leucoplasts and abundant smooth endoplasmic reticulum (SER; Fahn, 2000; Turner et al., 2000b). The secretion process is efficient, in that filling of the large extracellular pocket (the subcuticular oil storage space [SCS]) requires only approximately 25 h (Turner et al., 2000a). Therefore, peppermint peltate gland cells have the potential to serve as an excellent

[1] This work was supported by the U.S. Department of Energy, the Mint Industry Research Council, and the Washington State University Agricultural Research Center (Project 0268).

* Corresponding author; e-mail croteau@wsu.edu; fax 1–509–335–7643.

Article, publication date, and citation information can be found at www.plantphysiol.org/cgi/doi/10.1104/pp.104.050229.

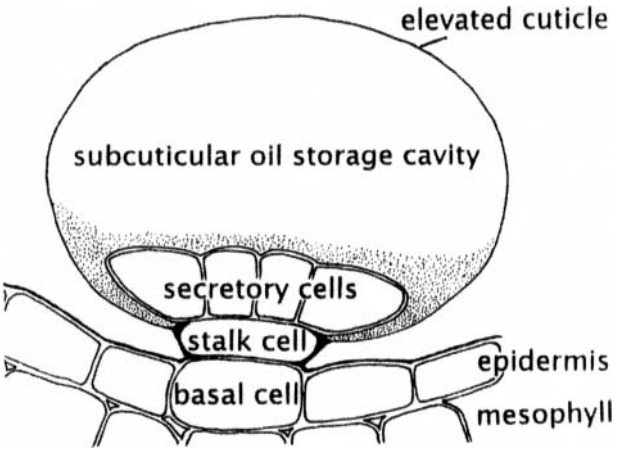

Figure 1. Schematic of a peltate glandular trichome of peppermint.

model for the cell biology of plant oil glands, supported by the established molecular genetics and enzymology of (−)-menthol biosynthesis. Determining the subcellular organization of monoterpene biosynthesis is an important step in understanding how these highly specialized secretory cells function.

We previously described the immunocytochemical localization of (−)-4*S*-limonene synthase (the committed step of the pathway; Fig. 2) to the stroma of peppermint glandular trichome leucoplasts (Turner et al., 1999). Here we present the subcellular localizations of four additional enzymes that mediate major steps of *p*-menthane monoterpene biosynthesis (Fig. 2): geranyl diphosphate synthase (GPPS, the prenyltransferase that condenses IPP and DMAPP to produce the C_{10} precursor of (−)-limonene), spearmint (*Mentha spicata*) limonene-6-hydroxylase (L6OH, for the regiospecific hydroxylation of limonene; in peppermint, the related limonene-3-hydroxylase produces isopiperitenol), isopiperitenol dehydrogenase (IPD, for the oxidation of isopiperitenol to isopiperitenone), and pulegone reductase (PR, catalyzing the reduction of the $\Delta^{4,8}$ double bond to produce menthone on route to menthol). With the exception of GPPS, these are the first localizations for these enzymes in plants, and the first localizations of any steps in a monoterpene biosynthetic pathway later than the early step of ring closure catalyzed by monoterpene synthases. Monoterpene biosynthesis is known to initiate in plastids (Eisenreich et al., 1997; Turner et al., 1999; Tholl et al., 2004), but in addition, we localized enzymes to

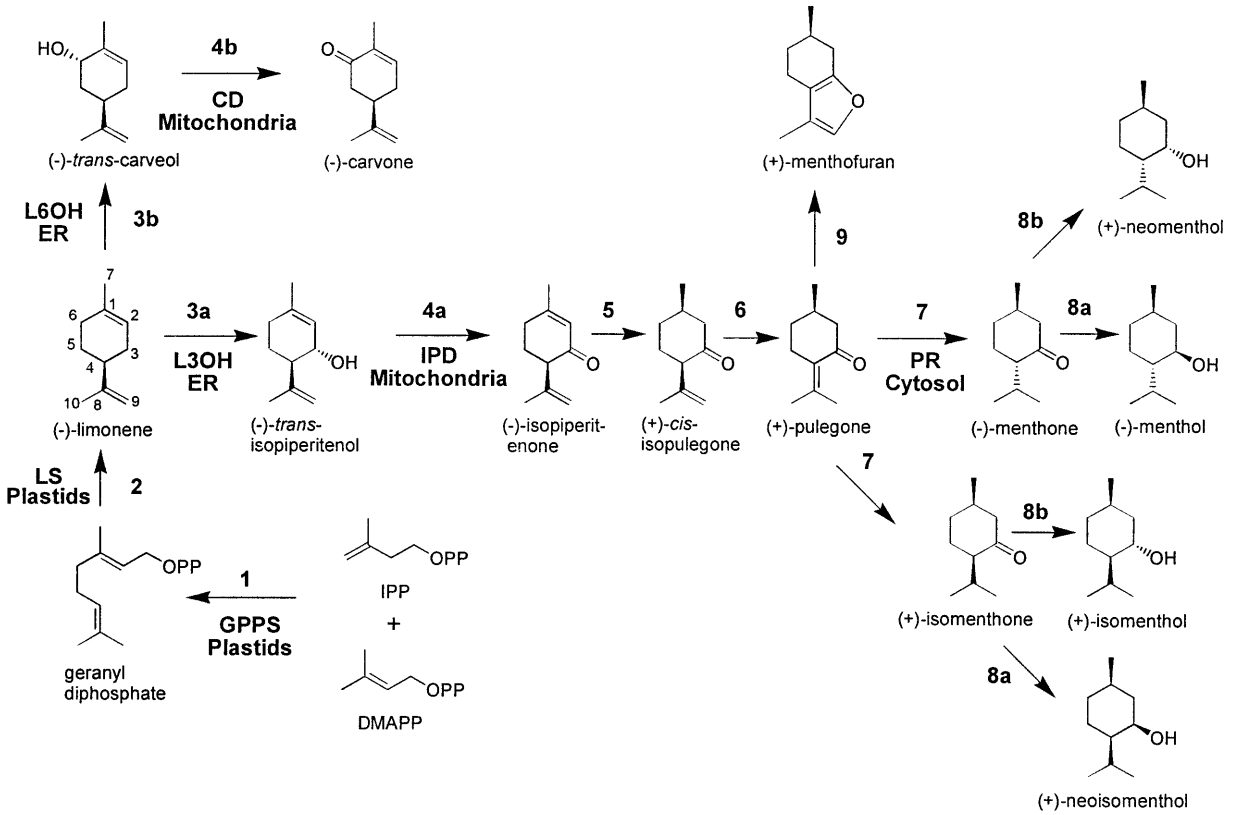

Figure 2. The monoterpene biosynthetic pathways in peppermint and spearmint. The enzymatic steps are catalyzed by: 1, GPPS; 2, (−)-limonene synthase (LS); 3a, (−)-limonene-3-hydroxylase (L3OH, peppermint); 3b, (−)-L6OH (spearmint); 4a, (−)-trans-IPD (peppermint); 4b, (−)-trans-CD (spearmint); 5, (−)-isopiperitenone reductase; 6, (+)-cis-isopulegone isomerase; 7, (+)-PR; 8a, (−)-menthone:(−)-menthol reductase; 8b, menthone:(+)-neomenthol reductase; and 9, (+)-menthofuran synthase. Subcellular locations are indicated.

endoplasmic reticulum, mitochondria, and the cytosol. We combine these observations with data relating to the monoterpene content of peppermint gland cells, the secretion rate, and monoterpene solubility to present a new model of monoterpene intracellular translocation and secretion.

RESULTS

Specificity of Affinity-Purified Antibodies

Western-blot analysis employing crude gland cell extracts of peppermint and spearmint indicated that after affinity purification the polyclonal antibodies to GPPS, L6OH, IPD, and PR used in this study labeled single protein bands corresponding to the correct M_rs for their target enzymes (Fig. 3).

GPPS Localization

The monoterpene biosynthetic pathway in peppermint (Fig. 2) initiates with the formation of the C_5 terpenoid precursors IPP and DMAPP derived from pyruvate and glyceraldehyde-3-phosphate by the plastidial nonmevalonate, methylerythritol phosphate (MEP) pathway (Eisenreich et al., 1997; Rodríguez-Concepción and Boronat, 2002). GPPSs are short-chain prenyltransferases that catalyze the condensation of IPP with its isomer DMAPP to form geranyl diphosphate (GPP; C_{10}), thereby directing isoprenoid pathway flux toward monoterpene (C_{10}) production (Tholl et al., 2001; Burke and Croteau, 2002). Peppermint GPPS is a heteromer composed of a 28-kD small subunit (SSU) and a 37-kD large subunit (LSU). The LSU deduced sequence shows considerable similarity to geranylgeranyl diphosphate synthase (GGPPS), sharing approximately 65% to 75% identity but is only approximately 25% identical to farnesyl diphosphate synthase. The SSU is more distinctive and shares only approximately 25% identity with GGPPS and approximately 17% identity with farnesyl diphosphate synthase. (Burke et al., 1999). Recently, similar heteromeric GPP synthases have been described from Antirrhinum and Clarkia flowers, with Antirrhinum and Mentha GPPS-SSUs sharing 53% deduced identity, and their GPPS-LSUs sharing 75% deduced identity (Tholl et al., 2004). Like the Mentha homologs, coexpressed recombinant Antirrhinum GPPS-SSU and GPPS-LSU produced GPP. Unlike the Mentha GPPS-LSU, the Antirrhinum GPPS-LSU showed GGPPS activity when expressed alone.

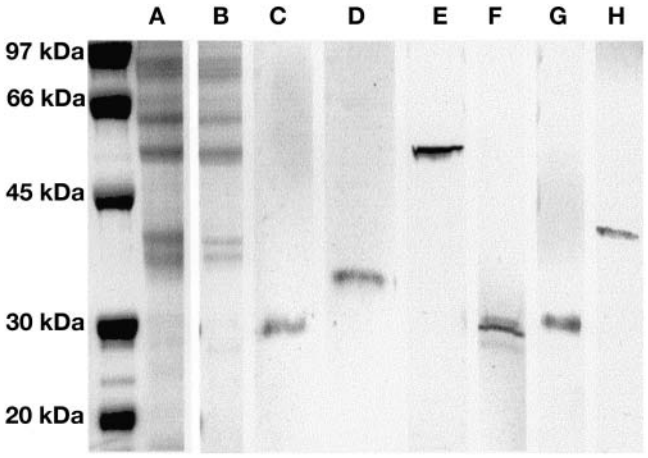

Figure 3. Immunoblots of peppermint or spearmint gland cell protein extracts demonstrating the specificity of affinity-purified antibodies. The far left lane presents molecular mass markers (5 μg/band). A, Representative SDS-PAGE of a peppermint gland cell protein extract (18 μg/lane). B, Representative SDS-PAGE of a spearmint gland cell extract (11 μg/lane). C, Immunoblotting with GPPS-SSU antibody (peppermint), (D) with GPPS-LSU antibody (peppermint), and (E) with (−)-L6OH antibody (spearmint). (−)-L6OH antibody labeling was absent from peppermint gland cell extracts. F, Immunoblotting with (−)-trans-IPD antibody (peppermint), (G) with (−)-trans-IPD antibody (spearmint), presumably labeling (−)-trans-carveol dehydrogenase, and (H) with (+)-PR antibody (peppermint). Protein bands were not detected with preimmune controls.

Presumably, the subcellular distribution of GPPS is an important factor affecting substrate allocation for the production of monoterpenes. The preprotein sequences of both the large and small subunits of Mentha GPPS contain probable N-terminal transit peptides (Burke et al., 1999), suggesting targeting to plastids (the site of the MEP pathway for precursor supply). Our immunocytochemical localizations confirm that, in peppermint, GPPS resides within the leucoplasts of the peltate glandular trichomes. Anti-GPPS-SSU antibodies specifically labeled secretory cell leucoplasts of secretory phase peppermint peltate glandular trichomes, with only background levels of labeling associated with other organelles within glandular cells (Fig. 4, A and B). Labeling was essentially absent from organelles of other cell types, including the large plastids of glandular trichome stalk cells (Fig. 4C), chloroplasts of mesophyll chlorenchyma (Fig. 4D), proplastids from young presecretory stage gland cells, and plastids of the small capitate glandular trichomes (Fig. 5E). Significant labeling was absent in the preimmune serum IgG controls (Fig. 4, E and F).

Within the leucoplasts, the GPPS-SSU label appeared to be frequently, but not consistently, associated with tubular plastid membranes. This was most apparent with chemically fixed glands for which staining more clearly contrasted tubular thylakoid membranes from stroma (Fig. 4A). With freeze-substituted plastids, the contrast between the tubules and the densely staining stroma was usually poor, often making the tubules especially difficult to distinguish. Figure 4B illustrates a small lobe of a freeze-substituted plastid within which the tubules are especially apparent.

GPPS-LSU was also localized to the leucoplasts of secretory phase glandular cells of the peltate glandular trichomes (Fig. 5A), but strong labeling also occurred within chloroplasts of mesophyll chlorenchyma cells adjacent to thylakoid membranes (Fig. 5B) and within the leucoplasts of small capitate glandular trichome secretory cells (Fig. 5D). The labeling in chloroplasts

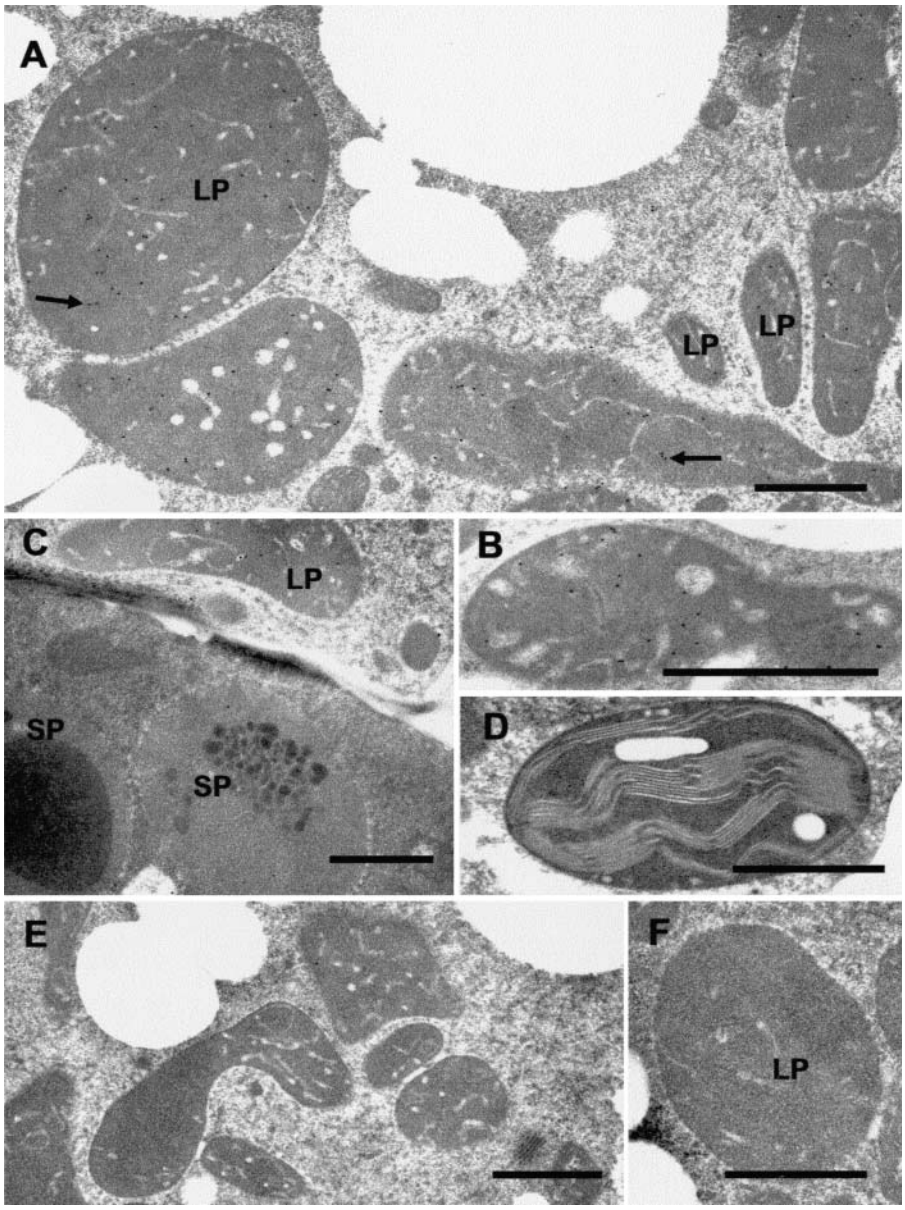

Figure 4. Immunocytochemical localization of GPPS-SSU in peppermint. A, Immunogold labeling of GPPS-SSU (small black dots, arrows) in leucoplasts in a secretory cell of peltate glandular trichomes. B, Immunogold labeling of a freeze-substituted secretory cell leucoplast with anti-GPPS-SSU. C, Portion of a peltate gland stalk cell (below) and an adjacent secretory cell (above) labeled with anti-GPPS-SSU. Labeling is absent from stalk cell plastids. D, Representative chloroplast in mesophyll parenchyma of anti-GPPS-SSU treated section. The chloroplast is unlabeled. E, Preimmune treatment of secretory-stage secretory cells. Leucoplasts are unlabeled. F, A leucoplast of a preimmune treated secretory cell. LP, Leucoplast; SP, stalk cell plastid. Bars = 1 μm.

and leucoplasts of capitate trichomes probably represents cross-labeling of another plastidial short-chain prenyltransferase, most likely GGPPS that shares 65% to 75% sequence identity with GPPS-LSU. The lack of labeling of capitate gland plastids by the GPPS-SSU antibody (Fig. 5E), and also by anti-limonene synthase antiserum (Turner et al., 1999), indicate the lack of essential biosynthetic enzymes in these structures and therefore suggest that the capitate trichomes of peppermint do not produce significant amounts of monoterpenes.

(−)-(4*S*)-Limonene Hydroxylase Localization

In Mentha, the majority of geranyl diphosphate produced by GPPS is cyclized by (−)-limonene synthase to form (−)-(4*S*)-limonene (Fig. 2; Colby et al., 1993). Mentha limonene synthase contains an N-terminal plastid targeting transit peptide and has been localized in peppermint to the stroma of leucoplasts from the secretory cells of peltate glandular trichomes (Turner et al., 1999). The product of this enzyme, (−)-(4*S*)-limonene, is regiospecifically and stereospecifically hydroxylated by cytochrome P450 limonene hydroxylases (Lupien et al., 1999; Wise and Croteau, 1999; Haudenschild et al., 2000). Different cytochrome P450 hydroxylases operate in different mint species, producing characteristic regiospecific oxygenation patterns. In spearmint, L6OH specifically hydroxylates the C6 position of the olefin precursor to produce (−)-trans-carveol, which is then oxidized to (−)-carvone (the major constituent of spearmint essential oil) by carveol dehydrogenase. In peppermint, a sterile hybrid of spearmint (*M. spicata*), and water

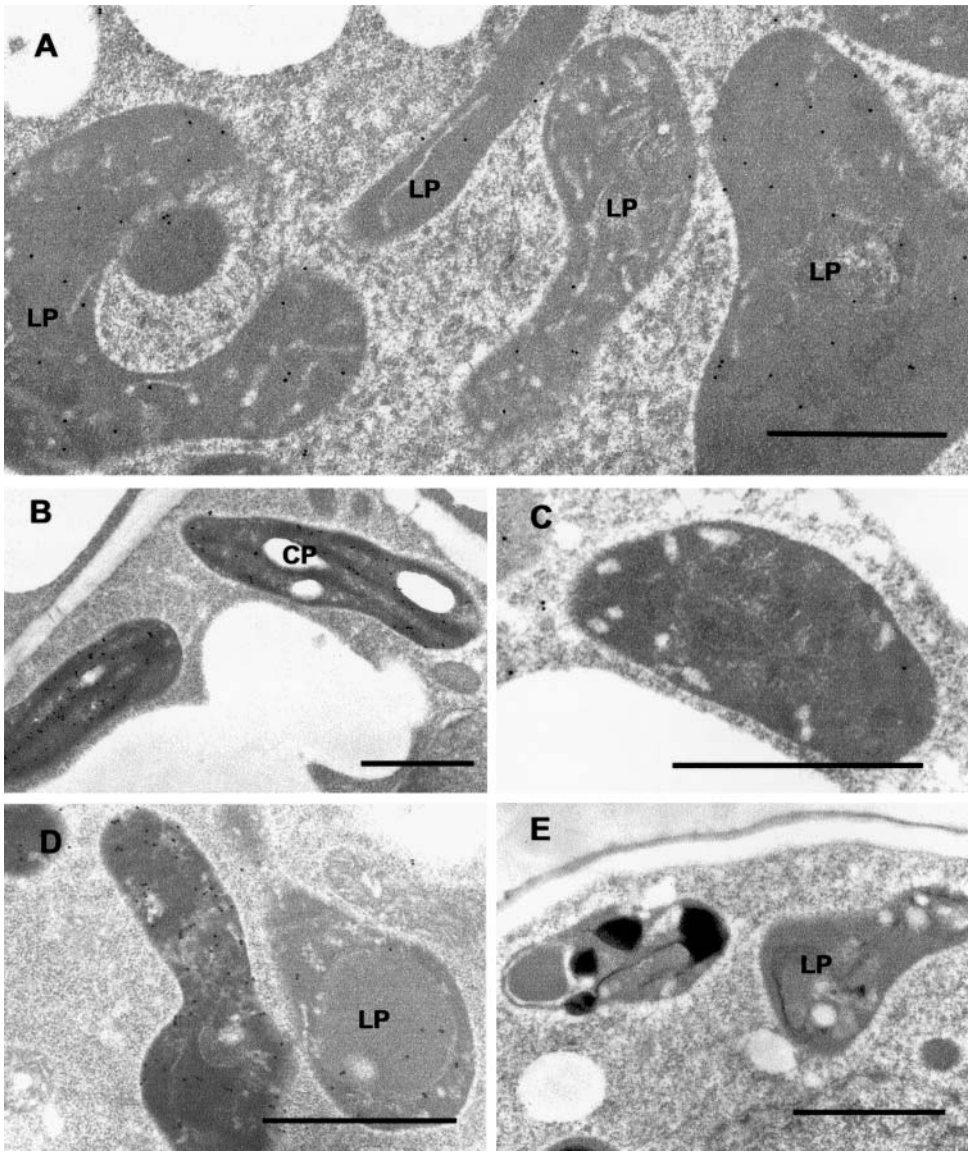

Figure 5. Immunocytochemical localization of the GPPS-LSU in peppermint. A, Immunogold labeling of GPPS-LSU (small black dots) in leucoplasts in a secretory cell of a peltate glandular trichome. B, Anti-GPPS-LSU labeled chloroplasts of mesophyll parenchyma. C, Normal rabbit serum IgG control showing an unlabeled leucoplast of a peltate gland secretory cell. D, Anti-GPPS-LSU labeled leucoplasts from a capitate glandular trichome. E, A secretory cell from a capitate glandular trichome treated with anti-GPPS-SSU IgG. Capitate gland leucoplasts are unlabeled. LP, Leucoplast; CP, chloroplast. Bars = 1 μm.

mint (*Mentha aquatica*), the C3 position of (−)-(4*S*)-limonene is specifically hydroxylated by (−)-(4*S*)-limonene-3-hydroxylase to form (−)-trans-isopiperitenol, which undergoes several subsequent redox transformations to produce the C3-oxygenated *p*-menthanes [e.g. (−)-menthol] characteristic of peppermint oil (Fig. 2). The amino acid sequences of these two limonene hydroxylases share about 70% identity (Lupien et al., 1999; Wüst et al., 2001); nevertheless, the available anti-L6OH polyclonal antibodies do not cross-react with peppermint limonene-3-hydroxylase, thereby necessitating the localization of L6OH in spearmint as a representative mint limonene hydroxylase.

Immunocytochemical localization of L6OH in spearmint is shown in Figure 6. Labeling occurred in the cap cells of secretory phase peltate glandular trichomes (Fig. 6, A and B) but was absent from all other cell types and tissues. Labeling was consistent with the association with SER (Fig. 6A). Preservation of spearmint glandular cells by conventional tissue fixation was poor, but it was adequate to determine the subcellular location of the enzyme. Intense labeling occurred in basal regions of the glandular cells near leucoplasts, as well as along the cell periphery, but very little labeling occurred adjacent to vacuoles in distal regions of the cells (Fig. 6B). Our immunolocalizations of L6OH are entirely consistent with predictions based on sequence analysis. PSORT (Nakai and Horton, 1999), TargetP (Emanuelsson et al., 2000), DAS (Cserzö et al., 1997), and TMHMM (Krogh et al., 2001) strongly indicate that L6OH is a membrane bound ER protein bearing a typical N-terminal membrane insertion sequence.

IPD Localization

In peppermint, (−)-trans-isopiperitenol is oxidized by (−)-trans-IPD to produce the ketone (−)-isopiperitenone (Fig. 2), while a nearly identical enzyme

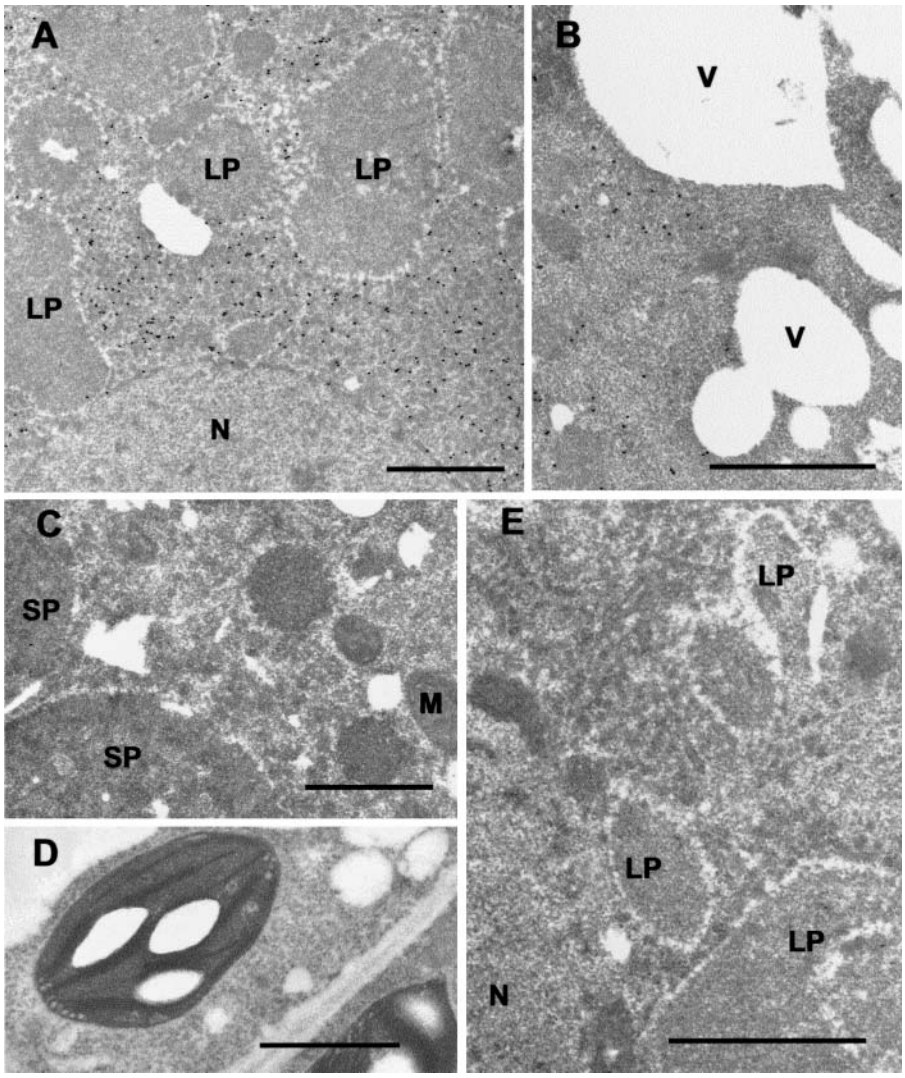

Figure 6. Immunocytochemical localization of (−)-(4*S*)-L6OH in spearmint. A, Immunogold labeling of L6OH (small black dots) in a secretory cell of a peltate glandular trichome. Abundant labeling is associated with SER and is absent from other organelles. B, Immunogold labeling of L6OH in a secretory cell of a peltate glandular trichome. Label intensity is reduced in regions adjacent to vacuoles. C, Immunogold labeling of L6OH in a stalk cell of a peltate glandular trichome. The SER is unlabeled. D, Anti-L6OH stained mesophyll parenchyma cell of spearmint leaf. All organelles are unlabeled. E, Preimmune control treatment of a secretory cell of a peltate glandular trichome. No labeling is evident. LP, Leucoplast; M, mitochondrion; N, nucleus; SP, stalk cell plastid; V, vacuole. Bars = 1 μm.

functions in spearmint to oxidize the C6 hydroxyl of (−)-trans-carveol to (−)-carvone, the major constituent of spearmint oil. Peppermint IPD is an operationally soluble 27-kD, pyridine nucelotide-dependent, short-chain dehydrogenase with a pH optimum of 10.5 and a strong preference for NAD as cofactor (K. Ringer, E. Davis, and R. Croteau, unpublished data; Kjonaas et al., 1985). The positively charged N-terminal sequence of IPD was identified as a possible mitochondrial targeting peptide by iPSORT (Bannai et al., 2002) and Predotar (http://www.inra.fr/predotar/) but not by TargetP (Emanuelsson et al., 2000) or PSORT (Nakai and Horton, 1999). The immunocytochemical localization of IPD presented here confirms a mitochondrial location.

Affinity-purified anti-IPD strongly labeled mitochondria of secretory stage glandular cap cells of peppermint peltate glandular trichomes (Fig. 7, A and B), whereas very little labeling was seen in presecretory stage gland cells. Mitochondria of other cell types were unlabeled, including those of the stalk cells (not shown) and adjacent mesophyll parenchyma (Fig. 7D). A similar pattern was seen with spearmint glands with labeling of secretory-stage gland cell mitochondria (Fig. 7C). Presumably, this labeling represents carveol dehydrogenase (CD) because the amino acid sequences of spearmint CD and peppermint IPD share 99% identity (K. Ringer, E. Davis, and R. Croteau, unpublished data).

Following the oxidation of (−)-trans-isopiperitenol by IPD, the endocyclic-double bond of (−)-isopiperitenone is reduced by (−)-isopiperitenone reductase to yield (+)-cis-isopulegone. An isomerase then mediates the shift of the $\Delta^{8,9}$ double bond of (+)-cis-isopulegone to the $\Delta^{4,8}$ position to produce (+)-pulegone (Fig. 2).

PR Localization

(+)-PR is an operationally soluble 38-kD protein and a member of the medium-chain dehydrogenase/reductase superfamily, which catalyses the NADPH-dependent reduction of the $\Delta^{4,8}$ double bond of

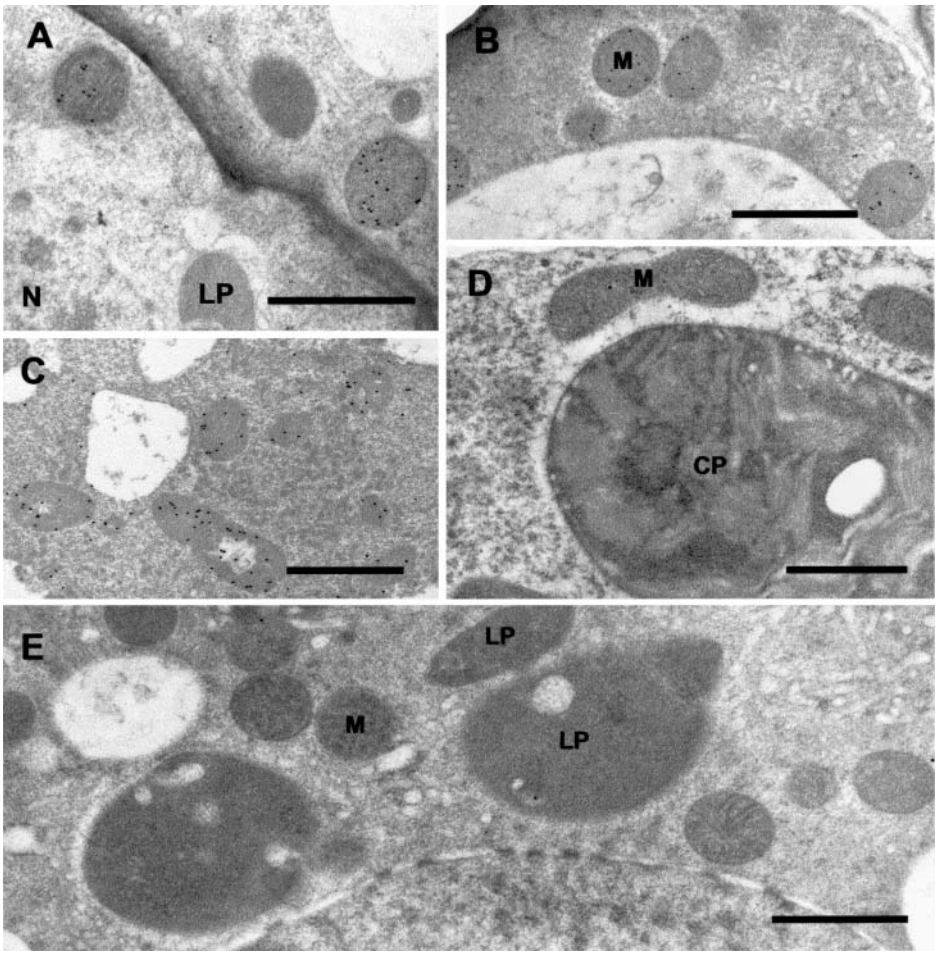

Figure 7. Immunocytochemical localization of (−)-trans-IPD in peppermint. A, Immunogold labeling of IPD (small black dots) in mitochondria in the basal region of a secretory cell of a peltate glandular trichome. B, Immunogold labeling of IPD in mitochondria in the peripheral region of a secretory cell of a peltate glandular trichome. C, Anti-IPD labeling of mitochondria in a secretory cell of a peltate glandular trichome from spearmint. Presumably CD (the spearmint ortholog of IPD) is labeled. D, Anti-IPD treatment of peppermint mesophyll parenchyma, in which mitochondria are unlabeled. E, Preimmune control treatment of a secretory cell of a peltate glandular trichome. CP, Chloroplast; LP, leucoplast; M, mitochondrion; N, nucleus. Bars = 1 μm.

(+)-pulegone to produce a 70:30 mixture of (−)-menthone and (+)-isomenthone (Fig. 2; Ringer et al., 2003). Like the other enzymes investigated in this study, abundant immunogold labeling of PR was restricted to secretory cells of peltate glandular trichomes. Abundant labeling occurred in the gland cell cytoplasm (Fig. 8, A and B) consistent with a soluble cytoplasmic enzyme and also occurred within secretory cell nucleoplasm (Fig. 8, B and C). Label was absent from all other cell types, including adjacent mesophyll parenchyma (Fig. 8, D and E). Preimmune controls were unlabeled (Fig. 8F). The significance of the nuclear labeling is unknown. A detoxification role analogous to that of animal NAD(P)H:quinone oxidoreductase 1 seems unlikely, because PR shows much greater substrate and cofactor specificity than would be expected for such a general function (Ringer et al., 2003; Talalay and Dinkova-Kostova, 2004).

DISCUSSION

We present the tissue and subcellular distributions of four essential enzymes of monoterpene biosynthesis in Mentha, peppermint GPPS, spearmint L6OH, peppermint IPD, and peppermint PR. The localizations of L6OH, IPD, and PR represent the first for any monoterpene biosynthetic enzymes downstream of the plastidial monoterpene cyclase, limonene synthase, and indicate the diversity of organelles involved in the biosynthetic process. At the tissue level, with the exception of GPPS-LSU, labeling for each of these enzymes was found only within glandular cap cells of secretory stage peltate glandular trichomes. This observation is consistent with the findings of McConkey et al. (2000) and Gershenzon et al. (2000) that monoterpene biosynthesis in peppermint is transcriptionally regulated, and that peak abundances of the relevant transcripts, enzymes, and activities and are associated with young leaves containing the highest surface densities of secretory stage peltate glands. The chloroplast labeling by the anti-GPPS-LSU antibody probably represents cross-reactivity with another plastidial prenyltransferase, most likely GGPPS with which GPPS-LSU shares greater than 70% identity (Burke et al., 1999). Since abundant anti-GPPS-SSU labeling occurred only in peltate glandular trichomes, functional GPPS heteromers must be restricted to the glandular cells. Although the plastids of the small capitate glandular trichomes were intensely stained

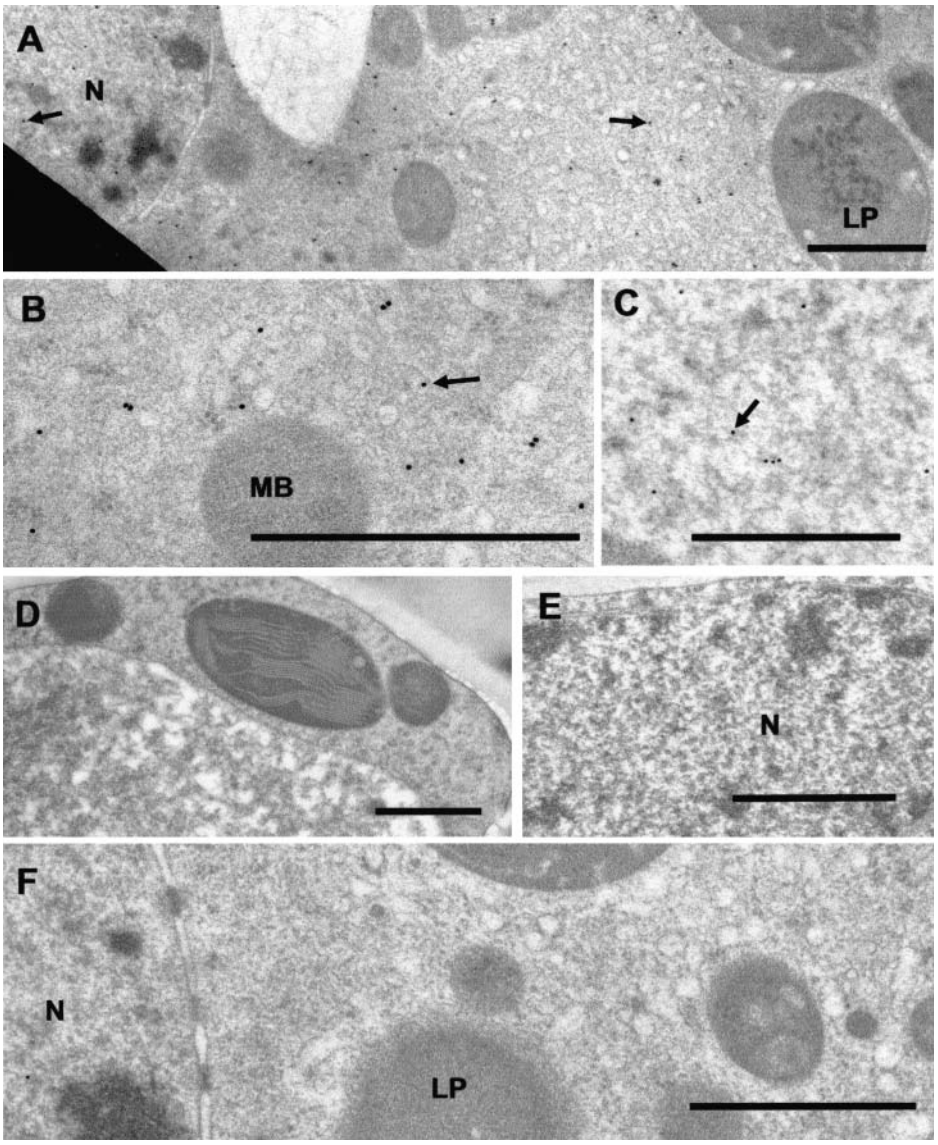

Figure 8. Immunocytochemical localization of (+)-PR in peppermint. A, Low magnification showing cytosolic and nuclear distribution of anti-PR immunogold label (small black dots, arrows). B, Higher magnification showing cytosolic anti-PR immunogold labeling within a secretory cell (arrow). C, Anti-PR immunogold labeling within the nucleoplasm of a secretory cell (arrow). D, Anti-PR IgG treatment of a mesophyll parenchyma cell showing unlabeled cytoplasm. E, Anti-PR IgG treatment of a mesophyll parenchyma cell showing unlabeled nucleoplasm. F, Preimmune control treated secretory cell of a peltate glandular trichome. Cytoplasm and nucleus are unlabeled. LP, Leucoplast; MB, microbody; N, nucleus. Bars = 1 μm.

by the anti-GPPS-LSU antibodies, they were not labeled by antibodies against GPPS-SSU or limonene synthase (Turner et al., 1999), indicating that the capitate glands do not produce significant amounts of monoterpenes.

Our immunocytochemical localizations demonstrated a high degree of compartmentalization within the glandular cells, with GPPS localized to gland cell leucoplasts, spearmint limonene-6-hydroxylase associated with SER membranes, IPD found within the mitochondrial matrix, and the apparently soluble PR occurring as a cytoplasmic enzyme. The plastid localization of GPPS was expected because the preproteins of both GPPS subunits contain predicted N-terminal plastid targeting transit peptides (Burke et al., 1999) and because the substrates, IPP and DMAPP, are derived from the plastidial MEP pathway (Eisenreich et al., 1997). GPPS also provides substrate to the plastidial enzyme (−)-limonene synthase to form (−)-limonene (the committed pathway step; Turner et al., 1999). The ER localization of limonene-6-hydroxylase is consistent with the ER targeting, membrane insertion sequence of this enzyme, and with its demonstrated microsomal association upon cellular fractionation (Lupien et al., 1999). The N-terminal targeting of IPD was ambiguous and its mitochondrial localization was unexpected.

Previous studies have provided substantial evidence that monoterpene biosynthesis is initiated within gland cell plastids but little evidence for the involvement of other organelles. Thus, a correlation was found between the presence of leucoplasts in glandular cells and the presence of monoterpenes in the gland secretions (Cheniclet and Carde, 1985). Studies employing isolated plant leucoplasts or chromoplasts demonstrated that these specialized plastids are capable of producing monoterpene hydrocarbons in vitro when provided with IPP (Gleizes et al., 1983;

Mettal et al., 1988; Pérez et al., 1990; Soler et al., 1992). In addition, ^{13}C-labeling experiments with basic precursors have indicated that plant monoterpenes are derived from the plastid localized MEP pathway (Eisenreich et al., 1997; Lichtenthaler, 1999; Rodríguez-Concepción and Boronat, 2002). Previous immunocytochemical localization of peppermint (−)-limonene synthase established that this key enzyme is present only within secretory cell leucoplasts of the peltate glandular trichomes (Turner et al., 1999). Recently, Tholl et al. (2004) employed transmission electron microscopy immunocytochemistry to localize the Antirrhinum GPPS-SSU to plastids of Antirrhinum petal cells.

Bouvier et al. (2000) reported the immunofluorescence localizations for a putative homodimeric GPP synthase (AtGPPS, GenBank no. CAC16849.1), DXP synthase, a "monoterpene synthase," and GGPP synthase in several plant species. Although organelle targeting-sequence analysis programs consistently predict that the putative AtGPPS is targeted to mitochondria, Bouvier et al. (2000) localized all these enzymes to plastids, with strong labeling of mesophyll parenchyma chloroplasts in Arabidopsis, Pinus, and Citrofortunella, as well as strong labeling of secretory cell leucoplasts in Pinus and Citrofortunella. This seemingly abundant, constitutive expression of AtGPPS in chlorenchyma of diverse species contrasts with our findings for Mentha. It is possible that the reliance of Bouvier et al. (2000) on crude polyclonal antiserum could have compromised the specificity of their probes; false positive labeling artifacts associated with the use of crude antiserum have been described by (Tavares et al., 2002).

The subcellular compartmentalization of monoterpene biosynthesis in diverse locales within peppermint glandular cells presents questions concerning the coordinated intracellular movement of monoterpene metabolites between organelles during production and secretion. In speculating about this process, enzyme localization in the context of intracellular transport, possible oil secretion mechanisms, and the known monoterpene content of peppermint gland cells must be considered. The rate of oil secretion is moderately rapid, in that the glandular cells of a peltate glandular trichome secrete approximately twice their cellular volume when filling the subcuticular oil storage space in roughly 20 to 30 h (Turner et al., 2000a). This event translates to a SCS filling rate of approximately 1.7×10^{-2} ($\pm 0.3 \times 10^{-2}$) nmol h^{-1} gland^{-1}, and secretion flux across the plasma membrane of approximately 1.8×10^{-6} ($\pm 0.4 \times 10^{-6}$) nmol μm^{-2} h^{-1}.

The C3-oxygenated monoterpenes, such as menthol, have some water solubility (Weidenhamer et al., 1993), and their small size and hydrophobicity should allow them to easily partition into membranes. McCaskill et al. (1992) compared the monoterpene composition and yield within freshly isolated peppermint gland cells with the composition and yield of the secreted, stored oil; since some monoterpenes may have been lost during gland cell isolation, quantification should be viewed as minimal estimates. McCaskill et al. (1992) presented oil compositional data averaged over 1×10^6 gland cell clusters (i.e. the disc of eight glandular cells of a peltate trichome). Assuming the volume of a peppermint gland cell disc (a squat cylinder 60 μm diameter $\times$ 16 μm high; Turner et al., 2000b) is approximately 4.5×10^{-5} μL, these data yielded an estimate of the average concentrations of monoterpene metabolites within the gland cells (Table I).

Published aqueous solubility estimates for monooxygenated monoterpenes vary widely (Fichan et al., 1999), but with the exception of limonene, water solubility of the monoterpene metabolites appears to be similar to, or greater than, our estimated values for their concentrations in gland cells (Weidenhamer et al., 1993; Fichan et al., 1999). Therefore, simple diffusion could play an important role in subcellular monoterpene translocation.

The water solubility of limonene is very low (<0.15 mM) compared to the solubilities of its C3-oxygenated derivatives (>1–5 mM; Weidenhamer et al., 1993; Fichan et al., 1999). If limonene accumulates, transmission electron microscopy should reveal osmium-stained pools of this lipid-like material at sites of accumulation within the gland cells. Although GPPS and limonene synthase (Turner et al., 1999) are clearly localized to peppermint gland cell leucoplasts, apparent lipid deposits do not collect within these organelles. Rather, lipid-like material accumulates along adjacent ER (periplastic ER) and to a lesser extent along the leucoplast outer membrane (Turner et al., 2000b). Therefore, it appears that once limonene is formed within peppermint gland cell leucoplasts, it is promptly exported from this site of biosynthesis. Perhaps the abundant ER-leucoplast membrane

Table I. *Estimated concentrations of selected monoterpene metabolites within peppermint glandular cells*

Estimated concentrations of monoterpene metabolites within glandular cells (bottom row) derived from the monoterpene content of isolated peppermint gland cell clusters (from McCaskill et al., 1992; top row) and an estimated volume of 4.5×10^{-5} μm for an eight-celled disk of secretory cells (gland cell cluster) from a typical peppermint peltate trichome. n.d., Not detectable.

	Limonene	Isopiperitenol	Isopiperitenone	Pulegone	Menthone	Menthol	Menthofuran
nmol/10^6 Gland cell clusters	290	n.d.	n.d.	14	386	5	240
Estimated concentration	3.2 mM	n.d.	n.d.	0.16 mM	4.29 mM	0.06 mM	2.67 mM

contacts (Turner et al., 2000b) facilitate transfer of limonene to the outer leaflet of ER membranes. At this locale, limonene-3-hydroxylase mediates hydroxylation of the olefin to produce (−)-trans-isopiperitenol.

Hydroxylation of monoterpene olefins greatly increases their water solubility (Weidenhamer et al., 1993; Li et al., 1998; Fichan et al., 1999), and the activity of mitochondrial IPD might produce a concentration gradient sufficient to drive rapid diffusion of (−)-trans-isopiperitenol into mitochondria. Alternatively, some type of terpenoid carrier protein, a mitochondrial membrane pump, or transient contacts between SER and mitochondrial membranes might facilitate isopiperitenol movement. Following oxidation, the next pathway step is mediated by isopiperitenone reductase, an operationally soluble, NADPH-dependent, short-chain reductase (Ringer et al., 2003) that lacks apparent targeting sequence information and is presumed to be cytosolic. Thus, it appears that (−)-isopiperitenone produced by mitochondrial IPD is immediately exported to the cytosol. Seemingly, the transfer of (−)-trans-isopiperitenol to the mitochondrial matrix, its conversion to (−)-isopiperitenone, and the subsequent export of (−)-isopiperitenone to the cytosol are very efficient, because neither (−)-trans-isopiperitenol nor (−)-isopiperitenone can be found in any but trace quantities in either the secreted oil or within the glandular cells (McCaskill et al., 1992). This rapid conversion occurs in spite of the widespread subcellular distribution of ER localized limonene-3-hydroxylase (which produces (−)-trans-isopiperitenol) and the relatively small volume occupied by the gland cell mitochondria (approximately 6% of cell volume; G. Turner and R. Croteau, unpublished data).

PR was localized to the cytosol, and preliminary immunocytochemical results indicate that menthone reductase is also cytosolic (G. Turner and R. Croteau, unpublished data); thus, the final steps of monoterpene biosynthesis in peppermint occur in the cytosol. Within peppermint glandular cells, most lipid-like deposits are associated with ER membranes. These deposits are especially abundant at ER of the peripheral cytoplasm, suggesting a directional movement of lipids (terpenoids) toward the secretory plasma membrane (Turner et al., 2000a, 2000b). If these lipid-like deposits represent the terminal monoterpene products, menthone and menthol, partitioned into ER membranes, then the abundant, direct ER-plasma membrane contacts (described in Turner et al., 2000b) could facilitate transfer of these monoterpenes from the ER to the plasma membrane. The mechanism of secretion is unknown, but an active process seems likely, primarily because the secretion is directional and because peppermint gland cell membranes show selectivity toward monoterpene types (McCaskill et al., 1992). For example, McCaskill et al. (1992) noted that 60% of the menthofuran produced in peppermint glands is selectively retained within the glandular cells. An ATP binding cassette (ABC) transporter would be a good candidate for such an essential oil pump. Putative ABC transporters are well represented in the peppermint gland expressed sequence tag library (Lange et al., 2000), and an inducible, plasma membrane, ABC transporter of the pleiotropic drug resistance subfamily has been implicated in diterpene secretion from tobacco epidermal cells (Jasiński et al., 2001). It is interesting to note that menthone stored in the SCS apparently remains in equilibrium with dissolved cytosolic menthone, because this ketone is converted to menthol by menthone reductase during the late postsecretion phase of gland development (McConkey et al., 2000). A more detailed investigation of menthone reductase and its role in monoterpene metabolism is in progress.

MATERIALS AND METHODS

Plant Materials, Secretory Cell Extracts, and Antibody Production

Peppermint (*Mentha* x *piperita* L. cv Black Mitcham) plants were grown with a 16-h photoperiod in a controlled environment chamber as previously described (Gershenzon et al., 2000). Spearmint (*Mentha spicata*) plants were grown with a 16-h photoperiod in a greenhouse with supplemental lighting from sodium vapor lights. Peltate glandular trichome secretory cells were isolated by a surface abrasion technique previously described (Gershenzon et al., 1992). The isolated glandular cells were sonicated three times for 30 s at 1/4 power with a VirTis (Gardiner, NY) Virsonic sonicator in a chilled 100 mM Na_2HPO_4-NaH_2PO_4, pH 7.4, buffer, containing 250 mM Suc, 5% (w/v) Amberlite XAD-4 resin, 1% PVPP-40, 1 mM dithiothreitol, 1 mM EDTA, and 1 mM benzamidine. The resulting lysates were filtered, homogenized with a glass homogenizer, and centrifuged for 30 min at 18,000*g*, followed by 90 min at 195,000*g* at 4°C. The resulting pellets and supernatants were employed for immunoblot analysis. Polyclonal antibodies, generated in rabbits against purified recombinant proteins (see below), were prepared by the contractor, Alpha Diagnostic International (San Antonio, TX).

Protein Purification and Production of Antibodies

Production of antibodies to recombinant L6OH (Lupien et al., 1999) and to both subunits of recombinant GPP synthase (Burke et al., 1999) was described previously. cDNAs encoding PR and IPD from a peppermint oil gland cell library (Lange et al., 2000; Ringer et al., 2003) were subcloned into pSBET (Schenk et al., 1995) and expressed in *Escherichia coli* BL21-CodonPlus cells (Stratagene, La Jolla, CA) by procedures previously described (Ringer et al., 2003). One-liter cultures were grown to A_{600} = 0.5 at 37°C in Luria-Bertani medium containing 50 μg kanamycin/mL, then induced with 1 mM isopropyl-β-D-thiogalactopyranoside and grown overnight at 15°C. The cells were then pelleted by centrifugation at 5,000 rpm, resuspended in chilled 50 mM MOPSO buffer, pH 7.5, that contained 1 mM benzamidine, and sonicated three times for 15 s at 1/4 power with a Virsonic sonicator (VirTis). The resulting lysate was centrifuged at 18,000*g* for 30 min, then at 195,000*g* for 90 min at 4°C, to afford the soluble enzyme fraction that was separated by chromatography on Source 30Q anion-exchange resin (Amersham Biosciences, Piscataway, NJ) with a salt gradient (0–1 M NaCl) in 50 mM MOPSO buffer, pH 7.5. The target enzymes, located by activity assay (Ringer et al., 2003), were then subjected to SDS-PAGE, and the corresponding proteins of the correct M_r were excised from the gels and used to generate antibodies in rabbits (Alpha Diagnostic International).

Partially purified recombinant PR obtained with Source 30Q anion-exchange chromatography, as described above, was further purified for use in affinity purification of polyclonal anti-PR antibodies. Source 30Q fractions demonstrating ample PR activity were combined and loaded onto a phenyl sepharose FPLC column (Amersham Biosciences) in a loading buffer containing final concentrations of 50 mM sodium phosphate buffer, 1 mM dithiothreitol, 10% (v/v) glycerol, and 1.5 M $(NH4)_2SO_4$. After washing with 10 mL of the loading buffer, proteins were eluted with a decreasing ammonium sulfate gradient [1.5–0 M $(NH4)_2SO_4$], and fractions were assayed for PR

activity (Ringer et al., 2003). Recombinant PR was then gel purified by SDS-PAGE to provide 99% pure PR for use in affinity purification of anti-PR antibodies.

The cDNA encoding IPD was also subcloned into the pBAD-TOPO vector (Invitrogen, Carlsbad, CA) and expressed in *E. coli* One Shot TOP10 cells (Invitrogen) to generate a fusion protein bearing a C-terminal His_6 tag. One-liter cultures were grown to an optical density of $A_{600} = 0.5$, induced with 0.1% Ara, and then grown overnight at 17°C. Soluble extracts were prepared as before, and the recombinant proteins were purified using a Ni-NTA agarose column (Qiagen USA, Valencia, CA) as per the manufacturer's instructions. The His_6-tagged recombinant protein (purity >95%) was then used for affinity purification of anti-IPD antibodies.

Antibody Affinity Purification

All crude antisera were affinity purified before use for immunocytochemistry. The total IgG fractions from antisera and preimmune sera were first isolated by FPLC using HiTrap Protein A affinity columns (Amersham Biosciences). Approximately 3 mL of serum was diluted with 7 mL of 20 mM sodium phosphate buffer, pH 7.5, then filtered and loaded onto a 1-mL protein A column. After rinsing with 10 mL of 20 mM phosphate buffer, the bound IgG was eluted with 2 mL of citric acid-sodium phosphate buffer, pH 3.5, and immediately neutralized with 120 μL of 1 M Tris-HCl, pH 9. The resulting antisera IgG fraction typically contained approximately 1 mg protein/mL. The IgG fraction was then affinity purified against the corresponding target protein. For this purpose, approximately 300 μg of the purified recombinant target enzyme was covalently linked to 0.5 mL (10^9 beads) of tosyl-activated M-280 magnetic dynabeads (Dynal A.S., Oslo) as per the manufacturer's instructions. Magnetic fields from small neodynium magnets were used to isolate the coated beads during antibody purification. Coated dynabeads were first suspended in a blocking solution of 3% bovine serum albumin (BSA) in Tris-buffered saline containing Tween 20 (TBST; 10 mM Tris-HCl, pH 7.5, 250 mM NaCl, and 0.3% Tween 20) for 2 to 4 h at 4°C, and then incubated overnight at 4°C in a solution containing 300 μL of protein A purified antisera IgG and 1.2 mL of the BSA-TBST blocking solution. The beads were then rinsed three times for 10 min each with TBST and finally with H_2O before eluting the bound IgG with 300 μL of Gly-HCl buffer, pH 2.5, for 45 s. The IgG solution was immediately neutralized with 30 μL of 1 M Tris-HCl, pH 8.5. The affinity-purified IgG solution was then centrifuged at 10,000*g* for 5 min to remove any remaining protein-coated dynabeads.

Immunoblots

Immunoblots were performed to test the specificity of antibodies toward the target enzymes (Fig. 3). Secretory cell protein extracts were separated using one-dimensional SDS-PAGE on 10% to 12% gels and then electroblotted to nitrocellulose according to instructions for the Bio-Rad (Hercules, CA) Mini-Protean Gel Electrophoresis and Mini-Transblot systems. The nitrocellulose blots were immersed for 2 to 4 h (room temp) or overnight (4°C) in a blocking solution containing either 5% nonfat dry milk in TBST, or 3% BSA in TBST. Blots were rinsed with TBST and then transferred to half strength blocking solution (2.5% dry milk or 1.5% BSA) containing a dilute solution of the purified primary antibody. Blots were incubated in primary antibody solutions for 4 h (room temp) or overnight (4°C). The blots were then rinsed three times (10 min each) in TBST and then transferred to a half strength blocking solution containing a 1:5,000 dilution of goat anti-rabbit antibodies conjugated to alkaline phosphatase. Blots were incubated with the secondary antibodies for 1 to 2 h (room temperature), then rinsed well with TBST and water prior to two 10-min rinses in alkaline phosphatase reaction buffer (0.1 M Tris-HCl, pH 9.5, with 0.1 M NaCl, and 5 mM $MgCl_2$). Antibody-labeled proteins were stained for several minutes in alkaline phosphatase reaction buffer containing 0.5 mg nitro-blue tetrazolium/mL and 0.17 mg 5-bromo-4-chloro-3-indolyl phosphate/mL to form dark deposits on the immunolabeled proteins. The reaction was stopped by washing blots with 20 mM Tris-HCl, pH 7.5, containing 0.5 mM EDTA.

Tissue Fixation and Sectioning

Rapid freezing, freeze-substitution, and embedment in LR White resin (Ted Pella, Redding, CA) of high-pressure frozen, freeze-substituted peppermint leaf tissues were performed in the Electron Microscopy Laboratory at the University of California, Berkeley. Small leaf discs, approximately 1 mm in diameter, from young peppermint leaves were rapidly frozen in a Balzers (BAL TEC AG, Balzers, Liechtenstein) model HPM 010 high pressure freezer and then freeze-substituted at −90°C for 72 h in a Leica (Wetzler, Germany) AFS automatic freeze substitution device. The freeze-substitution fluid consisted of anhydrous acetone containing 0.25% uranyl acetate, 0.1% glutaraldehyde, and 0.01% OsO4. After warming slowly to room temperature, the acetone mixture was exchanged for ethanol, and the ethanol was then exchanged for LR White resin in a short, graded series of steps. Infiltration with LR White resin was allowed to proceed overnight at room temp. The resin was then polymerized in a Pelco model 3440 research microwave oven (Ted Pella) at full power for 45 min.

Spearmint and some peppermint specimens were fixed by immersing 1-mm leaf discs overnight in a chilled (4°C) fixative solution containing 0.5% (v/v) glutaraldehyde, 2% (v/v) paraformaldehyde, and 50 mM PIPES buffer, pH 7.3. These specimens were then dehydrated in a graded ethanol series and infiltrated with LR White resin. After infiltration, the resin was allowed to polymerize overnight at 50°C in a conventional oven. Sectioning was accomplished using a Diatome (Diatome U.S., Hatfield, PA) diamond knife and a Leica Ultracut R ultramicrotome at the Washington State University Electron Microscopy Center. Silver sections were collected on uncoated 300-mesh nickel grids.

Immunocytochemistry

Thin sections on nickel grids were incubated for 1 to 2 h at room temp in a TBST blocking solution containing 1% (w/v) IgG-free BSA (Jackson ImmunoResearch Laboratories, West Grove, PA) and 1% (v/v) normal donkey serum. After blocking, specimens were transferred to a primary antibody solution containing TBST-BSA (0.5% IgG-free BSA) and either affinity-purified anti-serum IgG, or the equivalent concentration of the appropriate protein A purified preimmune IgG. The concentrations of the IgG solutions were determined by Bradford protein assays (Bio-Rad) using an IgG standard curve. Typically, each grid was incubated for 4 h room temp in 30 μL of solution containing 5 to 15 μg IgG/mL. After incubation with the primary antibody, the sections were rinsed a minimum of three times for 10 min with TBST, then transferred to a TBST blocking solution containing 2.5% to 5% colloidal gold conjugated donkey anti-rabbit secondary antibodies (Jackson ImmunoResearch). Sections were incubated for 1 to 2 h, rinsed with TBST, and followed by rinses with distilled water. After immuno-labeling, the immunogold-labeled sections were counter-stained for 12 min with a uranyl acetate-$KMnO_4$ solution consisting of 3 parts 2% aqueous uranyl acetate, and 1 part 1% $KMnO_4$, mixed and filtered immediately prior to staining (Franceschi et al., 1994). After thorough rinsing, the grids were coated with a thin film of Formvar (Electron Microscopy Sciences, Fort Washington, PA) to provide additional support to the sections. Stained sections were observed with a JEOL JEM 1200EX electron microscope and photographed with Kodak (Rochester, NY) electron microscopy film.

Protein Localization Prediction Algorithms

Protein sequences were examined for possible organelle targeting motifs with the following prediction programs: TargetP (Emanuelsson et al., 2000), ChloroP (Emanuelsson et al., 1999), and PSORT (Nakai and Horton, 1999), all available through the ExPASy (Expert Protein Analysis System) proteomics server (http://us.expasy.org/) sponsored by the Swiss Institute of Bioinformatics.

Estimate of Monoterpene Flux

Since both the dimensions of the glandular cells and the volume of the SCS are known (Turner et al., 2000a, 2000b), the flux of monoterpenes across the gland cell plasma membrane can be estimated. The SCS is a raised hemispherical pocket with a diameter of approximately 65 μm and a volume of approximately 7.2×10^{-5} μL. Taking 25 h (±5 h) for the filling time (Turner et al., 2000a) and assuming that the bulk of the secretion is composed of *p*-menthane monoterpenes with densities of approximately 0.9 g/mL, the filling rate is approximately 1.7×10^{-2} ($\pm 3.4 \times 10^{-3}$) nmol h^{-1} $gland^{-1}$. The disc of glandular cells can be approximated by a short cylinder 60 μm in diameter and 16 μm high, divided into eight cells by four lateral partitions. Assuming that most of the secretion exits the glandular cells along their outer and lateral walls, the secretory surface area (excluding the basal wall contacting the stalk cell) is approximately 9,700 μm^2. The flux of monoterpenes

across the secretory plasma membrane is then approximately 1.8×10^{-6} ($\pm 0.4 \times 10^{-6}$) nmol μm^{-2} h^{-1}.

Upon request, all novel materials described in this publication will be made available in a timely manner for noncommercial research purposes, subject to the requisite permission from any third-party owners of all or parts of the material. Obtaining any permissions will be the responsibility of the requestor.

ACKNOWLEDGMENTS

We thank Kent McDonald and the staff of the Electron Microscope Laboratory at the University of California, Berkeley, for assistance with freeze-substituted samples. We thank the staff of the Electron Microscopy Center at Washington State University for technical support, John Rogers for helpful discussions, Yujia Wu, Stefan Jennewein, Ed Davis, Kerry Ringer, and Charles Burke for helpful discussions and technical assistance, and Julianna Gothard for growing the plants.

Received August 2, 2004; returned for revision September 28, 2004; accepted September 29, 2004.

LITERATURE CITED

Bannai H, Tamada Y, Maruyama O, Nakai K, Miyano S (2002) Extensive feature detection of N-terminal protein sorting signals. Bioinformatics **18:** 298–305

Bouvier F, Suire C, d'Harlingue A, Backhaus RA, Camara B (2000) Molecular cloning of geranyl diphosphate synthase and compartmentation of monoterpene synthesis in plant cells. Plant J **24:** 241–252

Burke C, Croteau R (2002) Interaction with the small subunit of geranyl diphosphate synthase modifies the chain length specificity of geranylgeranyl diphosphate synthase to produce geranyl diphosphate. J Biol Chem **277:** 3141–3149

Burke CC, Wildung MR, Croteau R (1999) Geranyl diphosphate synthase: cloning expression and characterization of this prenyltransferase as a heterodimer. Proc Natl Acad Sci USA **96:** 13062–13067

Cheniclet C, Carde J-P (1985) Presence of leucoplasts in secretory cells and of monoterpenes in the essential oil: a correlative study. Isr J Bot **34:** 219–238

Colby SM, Alonso WR, Katahira EJ, McGarvey DJ, Croteau R (1993) 4*S*-Limonene synthase from the oil glands of spearmint (*Mentha spicata*): cDNA isolation characterization and bacterial expression of the catalytically active monoterpene cyclase. J Biol Chem **268:** 23016–23024

Cserzö M, Wallin E, Simon I, von Heijne G, Elofsson A (1997) Prediction of transmembrane α-helices in prokaryotic membrane proteins: the dense alignment surface method. Protein Eng **10:** 673–676

Degenhardt J, Gershenzon J, Baldwin IT, Kessler A (2003) Attracting friends to feast on foes: engineering terpene emission to make crop plants more attractive to herbivore enemies. Curr Opin Biotechnol **14:** 169–176

Dudareva N, Pichersky E (2000) Biochemical and molecular genetic aspects of floral scents. Plant Physiol **122:** 627–633

Eisenreich W, Sagner S, Zenk MH, Bacher A (1997) Monoterpene essential oils are not of mevalonoid origin. Tetrahedron Lett **38:** 3889–3892

Emanuelsson O, Nielsen H, Brunak S, von Heijne G (2000) Predicting subcellular localization of proteins based on their N-terminal amino acid sequence. J Mol Biol **300:** 1005–1016

Emanuelsson O, Nielsen H, von Heijne G (1999) ChloroP a neural network-based method for predicting chloroplast transit peptides and their cleavage sites. Protein Sci **8:** 978–984

Fahn A (1979) Secretory Tissues in Plants. Academic Press, London, pp 158–222

Fahn A (2000) Structure and function of secretory cells. Adv Bot Res **31:** 38–75

Fichan I, Larroche C, Gros JB (1999) Water solubility vapor pressure and activity coefficients of terpenes and terpenoids. J Chem Eng Data **44:** 56–62

Franceschi VR, Ding B, Lucas WJ (1994) Mechanism of plasmodesmata formation in characean algae in relation to evolution of intercellular communication in higher plants. Planta **192:** 347–358

Franceschi VR, Krekling T, Christiansen E (2002) Application of methyl jasmonate on *Picea abies* (Pinaceae) stems induces defense-related responses in phloem and xylem. Am J Bot **89:** 578–586

Gershenzon J, McCaskill D, Rajaonarivony JIM, Mihaliak C, Karp F, Croteau R (1992) Isolation of secretory cells from plant glandular trichomes and their use in biosynthetic studies of monoterpenes and other gland products. Anal Biochem **200:** 130–138

Gershenzon J, McConkey ME, Croteau RB (2000) Regulation of monoterpene accumulation in leaves of peppermint. Plant Physiol **122:** 205–213

Gleizes M, Pauly G, Carde J-P, Marpeau A, Bernard-Dagan C (1983) Monoterpene hydrocarbon biosynthesis by isolated leucoplasts of *Citrofortunella mitis*. Planta **159:** 373–381

Hallahan DL (2000) Monoterpenoid biosynthesis in glandular trichomes of labiate plants. Adv Bot Res **31:** 77–120

Harborne JB (1991) Recent advances in the ecological chemistry of plant terpenoids. *In* JB Harborne, FA Tomas-Barberan, eds, Ecology Chemistry and Biochemistry of Plant Terpenoids. Clarendon Press, Oxford, pp 399–426

Haudenschild C, Schalk M, Karp F, Croteau R (2000) Functional expression of regiospecific cytochrome P450 limonene hydroxylases from Mint (*Mentha* spp) in *Escherichia coli* and *Saccharomyces cervisiae*. Arch Biochem Biophys **379:** 127–136

Jasiński M, Stukkens Y, Degand H, Purnelle B, Marchand-Brynaert J, Boutry M (2001) A plant plasma membrane ATP binding cassette-type transporter is involved in antifungal terpenoid secretion. Plant Cell **13:** 1095–1107

Kjonaas RB, Venkatachalam KV, Croteau R (1985) Metabolism of monoterpenes: oxidation of isopiperitenol to isopiperitenone and subsequent isomerization to piperitenone by soluble enzyme preparations from peppermint (*Mentha piperita*) leaves. Arch Biochem Biophys **238:** 49–60

Krogh A, Larsson B, von Heine G, Sonnhammer ELL (2001) Predicting transmembrane protein topology with a hidden Markov model: application to complete genomes. J Mol Biol **305:** 567–580

Lange BM, Wildung MR, Stauber EJ, Sanchez C, Pouchnik D, Croteau R (2000) Probing essential oil biosynthesis and secretion by functional evaluation of expressed sequence tags from mint glandular trichomes. Proc Natl Acad Sci USA **97:** 2934–2939

Langenheim JH (1994) Higher-plant terpenoids-a phytocentric overview of their ecological roles. J Chem Ecol **20:** 1223–1280

Li J, Perdue EM, Pavlostathis SG, Araujo R (1998) Physicochemical properties of selected monoterpenes. Environ Int **58:** 353–358

Lichtenthaler HK (1999) The 1-deoxy-D-xylulose-5-phosphate pathway of isoprenoid biosynthesis in plants. Annu Rev Plant Physiol Plant Mol Biol **50:** 47–65

Lupien S, Karp F, Wildung M, Croteau R (1999) Regiospecific cytochrome P450 limonene hydroxylases from Mint (*Mentha*) species: cDNA isolation characterization and functional expression of (-)-4*S*-limonene-3-hydroxylase and (-)-4*S*-limonene-6-hydroxylase. Arch Biochem Biophys **368:** 181–192

Martin D, Tholl D, Gershenzon J, Bohlmann J (2002) Methyl jasmonate induces traumatic resin ducts, terpenoid resin biosynthesis and terpenoid accumulation in developing xylem of Norway spruce stems. Plant Physiol **129:** 1003–1018

McCaskill D, Gershenzon J, Croteau R (1992) Morphology and monoterpene biosynthetic capabilities of secretory-cell clusters isolated from glandular trichomes of peppermint (*Mentha piperita*). Planta **187:** 445–454

McConkey ME, Gershenzon J, Croteau RB (2000) Developmental regulation of monoterpene biosynthesis in the glandular trichomes of peppermint. Plant Physiol **122:** 215–223

Mettal U, Boland W, Beyer P, Kleinig H (1988) Biosynthesis of monoterpene hydrocarbons by isolated chromoplasts from daffodil flowers. Eur J Biochem **170:** 613–616

Nakai K, Horton P (1999) PSORT: a program for detecting the sorting signals of proteins and predicting their subcellular localization. Trends Biochem Sci **24:** 34–35

Pérez LM, Pauly G, Carde J-P, Belingheri L, Gleizes M (1990) Biosynthesis of limonene by the isolated chromoplasts from *Citrus sinensis* fruits. Plant Physiol Biochem **28:** 221–229

Pickett JA (1991) Lower terpenoids as natural insect control agents. *In* JB Harborne, FA Tomas-Barberan, eds, Ecology Chemistry and Biochemistry of Plant Terpenoids. Clarendon Press, Oxford, pp 297–313

Ringer KL, McConkey ME, Davis EM, Rushing GW, Croteau R (2003) Monoterpene double-bond reductases of the (-)-menthol biosynthetic pathway: isolation and characterization of cDNAs encoding (-)-isopiperitenone reductase and (+)-pulegone reductase of peppermint. Arch Biochem Biophys **418:** 80–92

Rodríguez-Concepción M, Boronat A (2002) Elucidation of the methylerythritol phosphate pathway for isoprenoid biosynthesis in bacteria and plastids. A metabolic milestone achieved through genomics. Plant Physiol **130:** 1079–1089

Schenk PM, Baumann S, Mattes R, Steinbiss H-H (1995) Improved high-level expression system for eukaryotic genes in *Escherichia coli* using T7 RNA polymerase and rare ^{Arg}tRNAs. Biotechniques **19:** 196–200

Soler E, Feron G, Clastre M, Dargent R, Gleizes M, Ambid C (1992) Evidence for a geranyl-diphosphate synthase located within the plastids of *Vitis vinifera* L cultivated *in vitro*. Planta **187:** 171–175

Steele CL, Lewinsohn E, Croteau R (1995) Induced oleoresin biosynthesis in grand fir as a defense against bark beetles. Proc Natl Acad Sci USA **92:** 4164–4168

Talalay P, Dinkova-Kostova AT (2004) Role of nicotinamide quinone oxidoreductase 1 (NQO1) in protection against toxicity of electrophiles and reactive oxygen intermediates. Methods Enzymol **382:** 355–364

Tavares R, Vidal J, van Lammeren A, Kreis M (2002) Non-purified anti-peptide sera generate tissue specific artifacts in immunohistochemical staining of *Arabidopsis thaliana*. Plant Sci **162:** 309–314

Tholl D, Croteau R, Gershenzon J (2001) Partial purification and characterization of the short-chain prenyltransferases geranyl diphosphate synthase and farnesyl diphosphate synthase from *Abies grandis* (grand fir). Arch Biochem Biophys **386:** 233–242

Tholl D, Kish CM, Oriova I, Sherman D, Gershenzon J, Pichersky E, Dudareva N (2004) Formation of monoterpenes in *Antirrhinum majus* and *Clarkia breweri* flowers involves heterodimeric geranyl diphosphate synthases. Plant Cell **16:** 977–992

Trapp S, Croteau R (2001) Defensive resin biosynthesis in conifers. Annu Rev Plant Physiol **52:** 689–724

Turner GW, Gershenzon J, Croteau RB (2000a) Distribution of peltate glandular trichomes on developing leaves of peppermint. Plant Physiol **124:** 655–663

Turner GW, Gershenzon J, Croteau RB (2000b) Development of peltate glandular trichomes of peppermint. Plant Physiol **124:** 665–679

Turner G, Gershenzon J, Nielson EE, Froehlich JE, Croteau R (1999) Limonene synthase, the enzyme responsible for monoterpene biosynthesis in peppermint, is localized to leucoplasts of oil gland secretory cells. Plant Physiol **120:** 879–886

Weidenhamer JD, Macias FA, Fischer NH, Williamson GB (1993) Just how insoluble are monoterpenes? J Chem Ecol **19:** 1799–1807

Wise ML, Croteau R (1999) Biosythesis of monoterpenes. *In* DE Cane, ed, Comprehensive Natural Products Chemistry, Vol 2, Isoprenoids Including Carotenoids and Steroids. Elsevier, Oxford, pp 97–153

Wüst M, Little DB, Schalk M, Croteau R (2001) Hydroxylation of limonene enantiomers and analogs by recombinant (-)-limonene 3- and 6-hydroxylases from mint (*Mentha*) species: evidence for catalysis within sterically constrained active sites. Arch Biochem Biophys **387:** 125–136